Eccentricity Severity Estimation of Induction Machines using a Sparsity-Driven Regression Model

Zheng, Xiangtian; Liu, Dehong; Inoue, Hiroshi; Kanemaru, Makoto

TR2022-126   October 12, 2022

Abstract

Eccentricity severity level estimation is of great importance in rotary machine fault detection. However, in practice machine operation conditions may influence the magnitude of fault signatures, making eccentricity severity estimation a challenging problem. In this paper, we develop a linear regression model incorporating multiple fault signature features to estimate the eccentricity severity level of induction machines under different operating conditions. In particular, the eccentricity severity level is modeled as a function of operating conditions and fault signature features including rotating speed, load torque, vibration, as well as current harmonics, etc, with corresponding weights to be determined. By imposing sparsity of weights, we learn from training data which dominant features have relatively larger impacts on the estimation. Experimental results show that our trained model exhibits satisfactory accuracy in quantitatively estimating eccentricity under various operation conditions.

The Fourteenth Annual Energy Conversion Congress and Exposition 2022

Eccentricity Severity Estimation of Induction Machines using a Sparsity-Driven Regression Model

Xiangtian Zheng, Dehong Liu
Mitsubishi Electric Research Laboratories
Cambridge, MA
zxt0515@tamu.edu, liudh@merl.com

Hiroshi Inoue, Makoto Kanemaru
Mitsubishi Electric Corporation
Amagasaki, Japan
{Inoue.Hiroshi, Kanemaru.Makoto}@cw.MitsubishiElectric.co.jp

Abstract—Eccentricity severity level estimation is of great importance in rotary machine fault detection. However, in practice machine operation conditions may influence the magnitude of fault signatures, making eccentricity severity estimation a challenging problem. In this paper, we develop a linear regression model incorporating multiple fault signature features to estimate the eccentricity severity level of induction machines under different operating conditions. In particular, the eccentricity severity level is modeled as a function of operating conditions and fault signature features including rotating speed, load torque, vibration, as well as current harmonics, *etc*, with corresponding weights to be determined. By imposing sparsity of weights, we learn from training data which dominant features have relatively larger impacts on the estimation. Experimental results show that our trained model exhibits satisfactory accuracy in quantitatively estimating eccentricity under various operation conditions.

Index Terms—Eccentricity, Fault detection, Induction machine, Sparsity model

I. Introduction

Eccentricity is one of the most common faults in rotary electric machines. For an eccentric machine, the axis of the rotor is not aligned with the axis of the stator, causing unbalanced air gap. In the case of the static eccentricity, the position of the minimal radial air-gap length is fixed in space. Study report shows that an inherent level of static eccentricity exists even in newly manufactured machines due to limits of manufacturing and assembly method [1]. If the rotor-shaft assembly is sufficiently stiff, the level of static eccentricity does not change. However, since static eccentricity causes a steady unbalanced magnetic pull in one direction, it may lead to bent rotor shaft and bearing wear and tear etc. Consequently, some degree of dynamic eccentricity will develop after long-time operation, where the position of minimum air gap rotates with the rotor during operation. Therefore, in reality, both static and dynamic eccentricities tend to co-exist in old induction machines [1], [2].

When there exists an eccentricity fault, the unbalanced air gap between the stator and the rotor causes degraded performance such as fluctuated torque and undesired vibrations [3]. In some situations, a serious eccentricity fault may lead to insulation damage or even sudden breakdown of the motor during operations [1]. Therefore, it is of great importance to detect eccentricity and examine the eccentricity level during

This work was finished when Xiangtian Zheng was an intern at MERL.

the manufacturing process for motor quality check and to monitor eccentricity severity during operation for preventive maintenance.

During past decades, motor eccentricity detection has attracted great attentions in the motor fault detection community, as summarized in [2], [4]. The most commonly used invasive method for eccentricity diagnosis is motor current signature analysis (MCSA) [1], [5]–[8], which aims to detect characteristic frequency components with respective to a certain type of eccentricity in the frequency spectrum.

For most induction machines with eccentricity fault, the signature frequency in the current signal is [8]

$$f_{ecc} = ((kR \pm n_d)\frac{1-s}{p} \pm \nu)f_s, \qquad (1)$$

where f_s is the fundamental supply frequency, R is the number of rotor slots, s is the slip, p is number of pole pairs, k is any positive integer, n_d is the eccentricity order ($n_d = 0$ in case of static eccentricity and $n_d = 1, 2, 3, ...$, in case of dynamic eccentriciy), and ν is the order of stator time harmonics. Without the number of rotor slots, a simplified version is given by

$$f_{ecc} = [1 \pm m(\frac{1-s}{p})]f_s = f_s \pm mf_r, \qquad (2)$$

where $f_r = \frac{1-s}{p}f_s$ is the rotor frequency related to the rotational speed.

Besides the conventional MCSA-based methods, researchers also explored signatures including higher order current harmonics [9], [10], vibrations [1], [11], stator voltage and current Park's vector [12], toque [13], *etc*. For example, For principal slot harmonic (PSH) type induction machines, who have a combination of pole pair number p and rotor slot number R that satisfy $R = 2p[3(m \pm q) \pm r]$, where $m \pm q = 0, 1, 2, ...$ and $r = 0, 1$, the conventional MCSA-based method does not work well since there is no significant dependency between current signals and eccentricity level. To deal with this issue, [9] introduces a frequency component $R(\frac{1-s}{p} + 1)f_s$ for the detection of static eccentricity level.

Other methods such as the magnetic field-based eccentricity detection are also explored [14]–[16], which aim to examine the magnitude of characteristic harmonics via analyzing the

spectrum of the stray flux. However, they are not widely accepted due to the costly installation of sensors.

In contrast to the binary eccentricity detection problem, eccentricity severity estimation is more challenging due to its complexity and the influence of operating conditions. Although a current spectrum-based indicator [17] is proposed to qualitatively assess the eccentricity level, there is no clear standardized criteria for quantitative estimation, especially under varying operation conditions. Based on our experience, the magnitude of fault signature frequency components may vary non-linearly, or even inversely proportional to the severity under certain load conditions. Therefore, it is desirable to propose a quantitative eccentricity estimation method for practical operation situations.

To tackle this problem, we propose a learning-based method that enables eccentricity estimation under different load conditions. We follow the principles of physics-informed machine learning [18] to steer the learning process towards identifying physically consistent solutions [19]–[21]. Our contribution in this paper lies in three aspects. First, we build a linear regression model of eccentricity severity as a function of multiple features of torque, vibration, and current harmonics, *etc.*, with weights to be learned with our training data. Second, we explore the importance of different features by imposing a sparsity constraint on weights of extracted features. Third, we estimate the severity of eccentricity levels under various load conditions with satisfactory results using our proposed method and learned model parameters.

II. PROBLEM FORMULATION

Inspired by prior knowledge of the physical model of induction machines and fault detection methods using different features, we aim to estimate eccentricity severity of induction machines by a learning-based method incorporating different eccentricity related features. Assume that we have N experiments conducted under different eccentricity levels and various load conditions. For each experiment, we obtain the eccentricity level, the load condition in torque, and multiple measurement time series including rotating speed, vibration acceleration, and three-phase current. By processing the measured data, we can obtain a feature matrix $\boldsymbol{X} \in \boldsymbol{R}^{N \times M}$ and a corresponding vector $\boldsymbol{y} \in \boldsymbol{R}^{N \times 1}$ of eccentricity levels represented by

$$\boldsymbol{X} = [\boldsymbol{x}_1, \cdots, \boldsymbol{x}_M], \tag{3}$$

$$\boldsymbol{y} = [y_1, \cdots, y_N]^T, \tag{4}$$

where $\boldsymbol{x}_i \in \boldsymbol{R}^{N \times 1}(i = 1, ..., M)$ corresponds to the ith feature and $y_j \geq 0$ $(j = 1, ..., N)$ is the eccentricity level defined by

$$y_j = \frac{d_j}{\delta_0} \times 100\%, \tag{5}$$

where d_j is the distance between the actual rotor axis and the stator axis, and δ_0 is the average air gap length in the corresponding healthy motor. For ideal healthy induction machines, the rotor and the stator are coaxial, therefore $d_j = 0$.

We model the eccentricity level as a function of operating conditions such as load, rotating speed, and vibration, *i.e.*, as well as the current spectral feature

$$\boldsymbol{y} = \boldsymbol{X}\boldsymbol{w} + \boldsymbol{u}, \tag{6}$$

where $\boldsymbol{w} = [w_1, ..., w_M]^T \in \boldsymbol{R}^{M \times 1}$ is a weight vector and $\boldsymbol{u}$ represents error.

To determine the feature vector $\boldsymbol{w}$, we have training data set $\{\boldsymbol{y}_T, \boldsymbol{X}_T\}$. Note that we only have limited data with a number of discrete eccentricity levels in $\boldsymbol{y}$. To avoid overfitting, we use a regularizer term on $\boldsymbol{w}$ and formulate the regression problem as an optimization problem

$$\boldsymbol{w}_T = \operatorname{argmin}_{\boldsymbol{w}} \frac{1}{2}||\boldsymbol{y}_T - \boldsymbol{X}_T \boldsymbol{w}||_2^2 + \alpha||\boldsymbol{w}||_1, \tag{7}$$

where α is a pre-defined coefficient of the regularization term and $||\boldsymbol{w}||_1 = \sum_{i=1}^{M} w_i$ represents the l_1 norm of $\boldsymbol{w}$. By minimizing the l_1-norm regularized objective function [22], we achieve a sparse solution of $\boldsymbol{w}$ that fits the regression model. Since $\boldsymbol{w}$ is sparse, meaning only a few non-zero coefficients in $\boldsymbol{w}$, the corresponding features play important roles in determining the eccentricity level.

To solve (7), we consider the augmented-Lagrangian scheme with penalty parameter ρ and variable $\boldsymbol{\mu}$

$$\mathcal{L}(\boldsymbol{w}, \boldsymbol{z}, \boldsymbol{\mu}) = \frac{1}{2}||\boldsymbol{y}_T - \boldsymbol{X}_T \boldsymbol{w}||_2^2 + \alpha||\boldsymbol{z}||_1 + \frac{\rho}{2}||\boldsymbol{w} - \boldsymbol{z} + \boldsymbol{\mu}||_2^2. \tag{8}$$

We then iteratively update $\boldsymbol{w}$, $\boldsymbol{z}$, and $\boldsymbol{\mu}$ using the alternating direction method of multipliers (ADMM) [23]. The detailed updating process is summarized in Algorithm 1.

Algorithm 1: ADMM for regularized linear regression model

Input: $\boldsymbol{X}_T$, $\boldsymbol{y}_T$, α, ρ, n_{iter};
Initialization: $\boldsymbol{z} \leftarrow \boldsymbol{z}_0, \boldsymbol{\mu} \leftarrow \boldsymbol{\mu}_0$;
for $j = 1, \ldots, n_{iter}$ **do**
    $\boldsymbol{w}_j \leftarrow \arg\min_{\boldsymbol{w}} \mathcal{L}(\boldsymbol{w}, \boldsymbol{z}_{j-1}, \boldsymbol{\mu}_{j-1})$,
    $\boldsymbol{z}_j \leftarrow \arg\min_{\boldsymbol{z}} \mathcal{L}(\boldsymbol{w}_j, \boldsymbol{z}, \boldsymbol{\mu}_{j-1})$,
    $\boldsymbol{\mu}_j \leftarrow \boldsymbol{\mu}_{j-1} + \boldsymbol{w}_j - \boldsymbol{z}_j$,
end
Output: $\boldsymbol{w_T} = \boldsymbol{w}_{n_{\text{iter}}}$.

Note that in each iteration, $\boldsymbol{w}_j$ has a closed-form solution which can be computed efficiently as

$$\boldsymbol{w}_j = (\boldsymbol{X}_T^T \boldsymbol{X}_T + \rho \boldsymbol{E}^T \boldsymbol{E})^{-1}(\boldsymbol{X}_T^T \boldsymbol{y}_T + \rho \boldsymbol{E}^T (\boldsymbol{z}_{j-1} - \boldsymbol{\mu}_{j-1})), \tag{9}$$

where $\boldsymbol{E} \in \boldsymbol{R}^{N \times N}$ is an identity matrix, and $\boldsymbol{z}_j$ can be solved by a soft-thresholding process as

$$z_{j,i} = \begin{cases} \boldsymbol{E}_i \boldsymbol{w}_j + \mu_{j,i} - \frac{\alpha}{\rho} & \text{if } \boldsymbol{E}_i \boldsymbol{w}_j + \mu_{j,i} \geq \frac{\alpha}{\rho} \\ \boldsymbol{E}_i \boldsymbol{w}_j + \mu_{j,i} + \frac{\alpha}{\rho} & \text{if } \boldsymbol{E}_i \boldsymbol{w}_j + \mu_{j,i} \leq -\frac{\alpha}{\rho} \\ 0 & \text{otherwise,} \end{cases} \tag{10}$$

where $z_{j,i}$ and $\mu_{j,i}$ are the ith element of $\boldsymbol{z}_j$ and $\boldsymbol{\mu}_j$, respectively, and $\boldsymbol{E}_i$ is the ith row vector of $\boldsymbol{E}$. Once we have learned

weight vector $\boldsymbol{w}_t$, we can estimate eccentricity severity level using

$$\boldsymbol{y}_t = \boldsymbol{X}_t \boldsymbol{w}_T \qquad (11)$$

with test data feature $\boldsymbol{X}_t$.

III. EXPERIMENTS

A. Setup

We show in Fig. 1 (a) a picture of our experiment setup and in Fig. 1 (b) an illustration diagram. To produce different eccentricity levels, the two original bearings between the rotor and the stator are taken out. Instead, two larger external bearings are used to support the rotor such that the motor's static eccentricity level can be manually adjusted within a certain range with high accuracy. A magnetic powder brake, whose torque can be tuned by changing its input operating current, is used as the load. The whole motor drive system is enclosed in a clear cage for safety purpose. During operation, multiple sensors are used to record synchronized time-sequence data: i) one tachometer measures the rotating speed, ii) two accelerometers record the motor vibration along horizontal and vertical directions respectively, and iii) three current probes records the three-phase stator current accordingly.
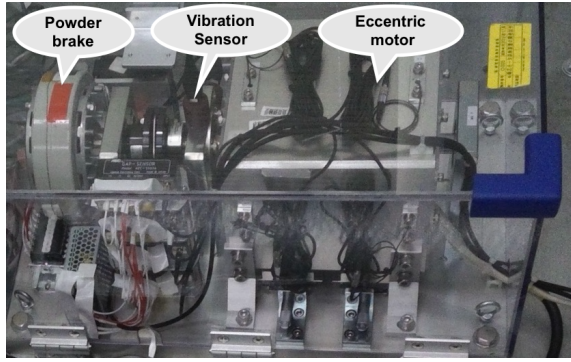
(a) Experiment setup
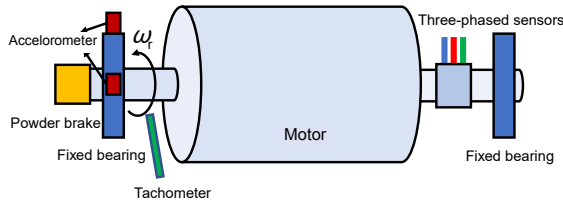
(b) Illustration diagram

Fig. 1. Experiment setup and its illustration diagram

Experiments are conducted under various conditions of eccentricity level and load by adjusting the external bearings and the input operating current of the magnetic powder brake. For each experiment, given a pair of eccentricity level and load, we follow three steps: i) shift the bearings that support the rotor to the eccentricity level under stationary state, ii) set the input current of the magnetic powder brake to provide desired load torque, and iii) start the motor and record data when the motor is running in steady status.

Specifically, we examine 5 different eccentricity levels in percentage as $y_j \in \mathcal{Y} = \{0\%, 11\%, 25\%, 43\%, 56\%\}$ and 8 different load conditions with torque $T_j \in \mathcal{T} = \{0.0, 0.3, 0.5, 0.9, 1.4, 2.0, 2.7, 3.5\}$ in Nm. Therefore, a total of 40 experiments, each under a unique pair of eccentricity level and load, are conducted with operating data collected for further analysis.

B. Data processing

To explore the relationship between motor operation features and eccentricity levels, we pre-process original measurements to fit the input of our regression model. For each experiment, we collect torque, time sequences of rotating speed, horizontal acceleration, vertical acceleration, and three-phase current, each of 60 seconds with a sampling rate of 10^4 Sa/s. To enrich the training and testing dataset, we first segment each time sequence of original 60-second measurements into 12 non-overlapped segments, each of 5 seconds, resulting a total of $N = 480$ datasets for all 40 experiments. Each dataset includes load torque, rotating speed, acceleration time sequence, and three-phase stator current sequences, *etc.* We then randomly pick half of the 480 datasets for training and the remaining half for testing. Data features of each dataset are extracted with details described as follows.

1) Average Vibration Velocity Calculation: We calculate the average vibration velocity as one feature, following three steps below.

- Integrate the vibration acceleration time series A_x and A_y independently to get the raw vibration velocity time series, using the function `cumtrapz` in MATLAB.
- Calculate the cumulative error-caused velocity trend by the moving average method, where the window size is set as 10 samples.
- Calculate the average absolute value of the net vibration velocity based on the detrended vibration velocity on horizontal and vertical directions.

Specifically, Fig. 2 plots an example of time series of acceleration measurements and detrended vibration velocity.

2) Eccentricity-related Stator Current Components Extraction: As indicated in equation (2), eccentricity-related stator current components involve the following characteristic harmonics of current spectrum,

$$f_k = f_s + kf_r, \ k = 0, \pm 1, \pm 2, \dots . \qquad (12)$$

where f_r is the rotational frequency. Considering perturbations in the actual rotating speed, we approximate the rotor rotational frequency range $[f_r^{min}, f_r^{max}]$ using the average rotating speed $\overline{\Omega}$ with some tolerance as

$$f_r^{min} = (\overline{\Omega} + b_1)/\Omega_0 \times (f_s/p), \qquad (13)$$
$$f_r^{max} = (\overline{\Omega} + b_2)/\Omega_0 \times (f_s/p), \qquad (14)$$

where Ω_0 is the nominal rotating speed, f_s is the supply frequency, p is the number of pole pairs, and b_1 and b_2 are pre-defined bias terms to amend the overestimation of the
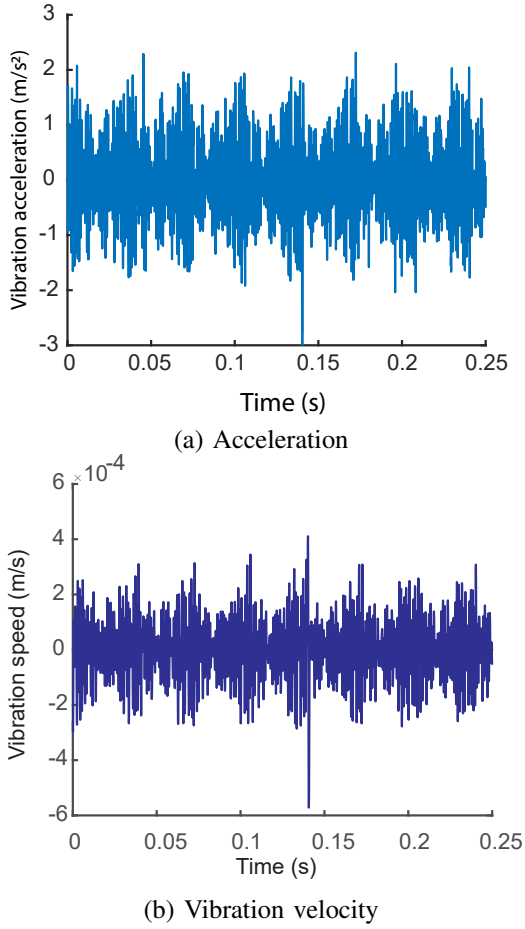
(a) Acceleration

(b) Vibration velocity

Fig. 2. Examples of (a) time series of acceleration and (b) vibration velocity.

(a) Stator current

(b) Frequency spectrum

Fig. 3. Examples of (a) Time series of stator current and (b) Frequency spectrum of stator current.

tachometer. In our case, $\Omega_0 = 1800\text{rpm}$, $f_s = 60\text{Hz}$, $p = 2$, $b_1 = -19\text{rpm}$, and $b_2 = -9\text{rpm}$.

Given the three-phase current, we first perform Fast Fourier Transform (FFT) on the current time series of each phase $H^P = \text{FFT}(I^P)$, where $P \in \{A, B, C\}$ represents one of the three phases. We then calculate the kth harmonic components H_k^P of each phase in the following way, where we set the maximum harmonic order $k_0 = 98$ and tolerance band Δf as 1.5 Hz.

$$H_k^P = \max(H^P(f) | f_k^{\min} \le f \le f_k^{\max}), \qquad (15)$$

where

$$\begin{aligned} f_k^{\min} &= f_s + k f_r^{\min} - \Delta f, \\ f_k^{\max} &= f_s + k f_r^{\max} + \Delta f, \\ k &= -1, 0, 1, \ldots, k_0. \end{aligned}$$

Finally, we calculate the magnitude of the eccentricity-related current components H_k by calculating the mean of three phases

$$\boldsymbol{H}_k = (H_k^A + H_k^B + H_k^C)/3. \qquad (16)$$

Fig. 3 plots examples of the collected time-domain stator current data and its corresponding frequency spectrum. We

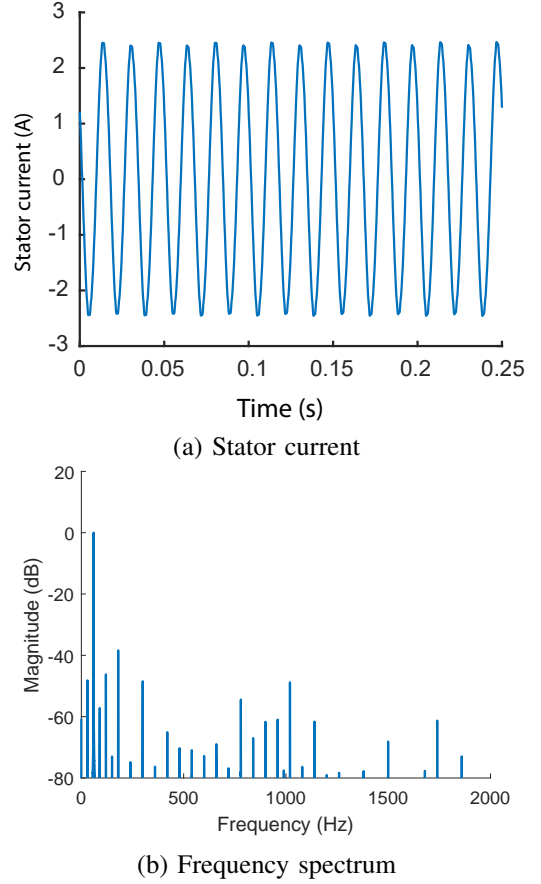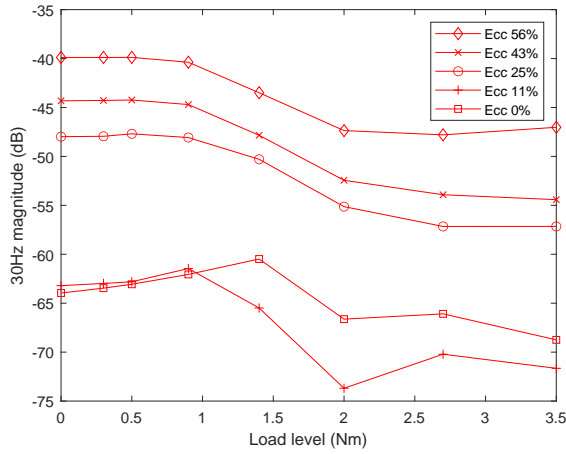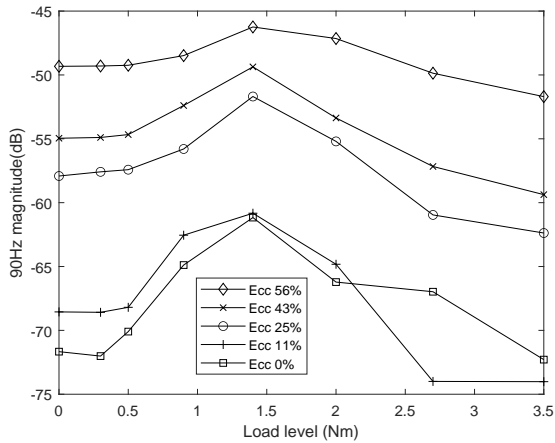can observe a bunch of rotor frequency harmonics with various magnitudes.

To further explore the harmonic magnitude, we plot in Fig. 4 the magnitude of 30Hz and 90Hz in current spectrum relative to the 60Hz operating frequency component with respect to different load conditions. We can observe that the magnitude may vary greatly with load, and not reliable for eccentricity severity level estimation, especially when the eccentricity level is relatively low. Therefore, it is not reliable to estimate the eccentricity severity level according to solely the magnitude of 30Hz or 90Hz.

Consequently, load torque, rotor speed, vibration acceleration, vibration speed, and current spectral features are provided for further model training and testing. In summary, data processing provides load torque $\boldsymbol{T} = [T_1, ..., T_j, ..., T_N]^T$ with $T_j \in \mathcal{T}$, rotating speed $\boldsymbol{\Omega}_r$, horizontal, vertical and total vibration acceleration $\boldsymbol{A}_x$, $\boldsymbol{A}_y$, and $\boldsymbol{A} = \sqrt{\boldsymbol{A}_x^2 + \boldsymbol{A}_y^2}$ respectively, horizontal, vertical and total vibration speed $\boldsymbol{V}_x$, $\boldsymbol{V}_y$, and $\boldsymbol{V} = \sqrt{\boldsymbol{V}_x^2 + \boldsymbol{V}_y^2}$, respectively, and current spectral features $\{\boldsymbol{H}_n\}$, formulated in feature matrix $\boldsymbol{X}$ as

$$\boldsymbol{X} = [\boldsymbol{T}, \boldsymbol{\Omega}_r, \boldsymbol{A}_x, \boldsymbol{A}_y, \boldsymbol{A}, \boldsymbol{V}_x, \boldsymbol{V}_y, \boldsymbol{V}, \boldsymbol{H}_{-1}, \boldsymbol{H}_1, ..., \boldsymbol{H}_{k_0}]. \qquad (17)$$

(a)

(b)

Fig. 4. Frequency component magnitude of (a) 30Hz and (b) 90Hz w.r.t. load

All features are normalized to have a unit variance to ensure all features are equally weighted without any prior knowledge. The feature correlation matrix is shown in Fig. 5. It is clear that acceleration related feature are related to each other and high order harmonics are also closely related to each other.

C. Algorithm Implementation and results

We implement Algorithm 1 in Matlab, with the pre-defined parameter $\alpha = 10$, $\rho = 10$, initial values $\boldsymbol{\mu}_0 = \mathbf{0}$, $\boldsymbol{z}_0 = \mathbf{0}$, and the number of training iterations $n_{\text{iter}} = 10^3$.

A plot of the sparse weights learned from our training data is shown in Fig. 6. We can see that 90Hz frequency component plays a dominant role in the severity level estimation. Besides the 90Hz frequency component, other features such as vibration and some high order harmonics also contribute to the final estimation. This agrees with literatures that use vibration and high-order harmonics for eccentricity detection.

The estimation results using trained model as well as the true eccentricity severity levels are shown in Fig. 7. We observe that our estimates of eccentricity levels match the true eccentricity setup well across all different load conditions.
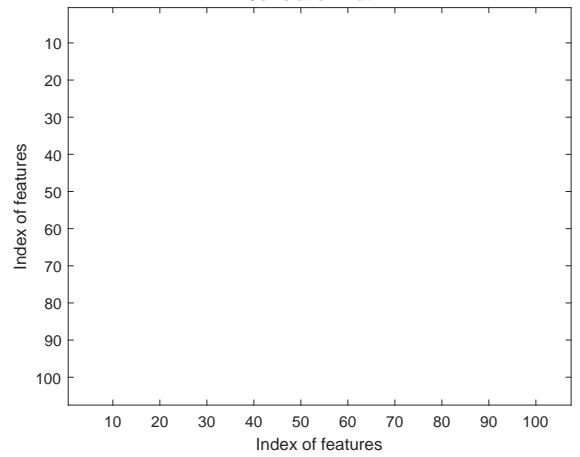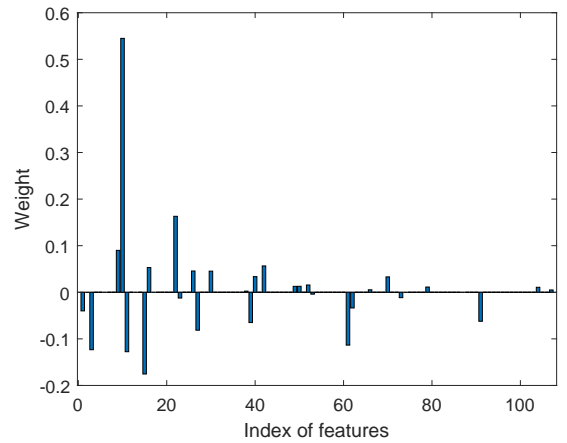

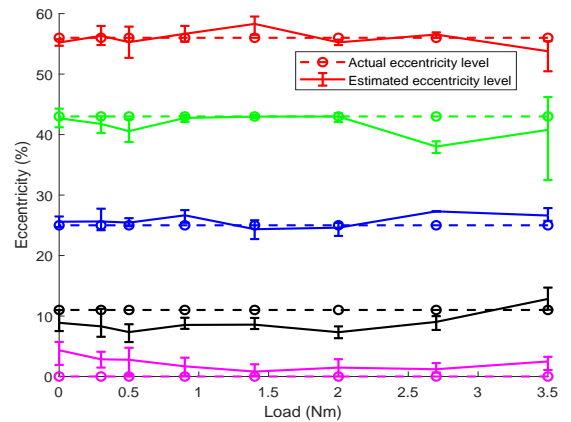Fig. 5. Feature correlation matrix

Fig. 6. Feature weights

Fig. 7. Eccentricity severity level estimation under various load conditions.

To quantify the model performance, we take the coefficient of determination [24] as the accuracy metric, which can be calculated as

$$R^2 := 1 - \frac{\sum_i (y_i - \hat{y}_i)^2}{\sum_i (y_i - \bar{y})^2}, \qquad (18)$$

where y_i represents the real value of the ith sample, $\hat{y}_i$ represents the estimated value, and $\bar{y}$ represents the mean of real values of all samples. We achieve the coefficient of determination value $R^2 = 0.981$, which is very close to the ideal value 1 when all estimates are exactly the same as the corresponding true eccentricity levels.

IV. CONCLUSION

We proposed a sparsity-driven linear regression model for induction machine eccentricity severity estimation under various operating conditions. By imposing sparsity, we explored important signatures that play important roles in severity estimation. Our experimental results validate the proposed model in quantitatively estimating eccentricity under various operation conditions with satisfactory accuracy.

.

REFERENCES

[1] D. G. Dorrell, W. T. Thomson, and S. Roach, "Analysis of airgap flux, current, and vibration signals as a function of the combination of static and dynamic airgap eccentricity in 3-phase induction motors," *IEEE Transactions on Industry applications*, vol. 33, no. 1, pp. 24–34, 1997.

[2] S. Nandi, H. A. Toliyat, and X. Li, "Condition monitoring and fault diagnosis of electrical motors—a review," *IEEE Transactions on energy conversion*, vol. 20, no. 4, pp. 719–729, 2005.

[3] A. Barbour and W. Thomson, "Finite element study of rotor slot designs with respect to current monitoring for detecting static airgap eccentricity in squirrel-cage induction motors," in *IAS'97. Conference Record of the 1997 IEEE Industry Applications Conference Thirty-Second IAS Annual Meeting*, vol. 1. IEEE, 1997, pp. 112–119.

[4] J. Faiz and S. Moosavi, "Eccentricity fault detection–from induction machines to DFIG—a review," *Renewable and Sustainable Energy Reviews*, vol. 55, pp. 169–179, 2016.

[5] M. El Hachemi Benbouzid, "A review of induction motors signature analysis as a medium for faults detection," *IEEE Transactions on Industrial Electronics*, vol. 47, no. 5, pp. 984–993, 2000.

[6] A. Bellini, F. Filippetti, C. Tassoni, and G.-A. Capolino, "Advances in diagnostic techniques for induction machines," *IEEE Transactions on industrial electronics*, vol. 55, no. 12, pp. 4109–4126, 2008.

[7] S. Nandi, R. M. Bharadwaj, and H. A. Toliyat, "Performance analysis of a three-phase induction motor under mixed eccentricity condition," *IEEE Transactions on Energy Conversion*, vol. 17, no. 3, pp. 392–399, 2002.

[8] S. Nandi, S. Ahmed, and H. A. Toliyat, "Detection of rotor slot and other eccentricity related harmonics in a three phase induction motor with different rotor cages," *IEEE Transactions on Energy Conversion*, vol. 16, no. 3, pp. 253–260, 2001.

[9] L. Zhou, B. Wang, C. Lin, H. Inoue, and M. Miyoshi, "Static eccentricity fault detection for psh-type induction motors considering high-order air gap permeance harmonics," in *2021 IEEE International Electric Machines & Drives Conference (IEMDC)*. IEEE, 2021, pp. 1–7.

[10] N. Arthur and J. Penman, "Induction machine condition monitoring with higher order spectra," *IEEE Transactions on Industrial Electronics*, vol. 47, no. 5, pp. 1031–1041, 2000.

[11] J. Cameron, W. Thomson, and A. Dow, "Vibration and current monitoring for detecting airgap eccentricity in large induction motors," in *IEE Proceedings B (Electric Power Applications)*, vol. 133, no. 3. IET, 1986, pp. 155–163.

[12] A. Cardoso and E. Saraiva, "Computer-aided detection of airgap eccentricity in operating three-phase induction motors by park's vector approach," *IEEE Transactions on Industry Applications*, vol. 29, no. 5, pp. 897–901, 1993.

[13] J. F. Bangura, R. J. Povinelli, N. A. Demerdash, and R. H. Brown, "Diagnostics of eccentricities and bar/end-ring connector breakages in polyphase induction motors through a combination of time-series data mining and time-stepping coupled fe-state-space techniques," *IEEE Transactions on Industry Applications*, vol. 39, no. 4, pp. 1005–1013, 2003.

[14] A. Ceban, R. Pusca, and R. Romary, "Study of rotor faults in induction motors using external magnetic field analysis," *IEEE Transactions on industrial electronics*, vol. 59, no. 5, pp. 2082–2093, 2011.

[15] O. Vitek, M. Janda, and V. Hajek, "Effects of eccentricity on external magnetic field of induction machine," in *Melecon 2010-2010 15th IEEE Mediterranean Electrotechnical Conference*. IEEE, 2010, pp. 939–943.

[16] O. Vitek, M. Janda, V. Hajek, and P. Bauer, "Detection of eccentricity and bearings fault using stray flux monitoring," in *8th IEEE Symposium on Diagnostics for Electrical Machines, Power Electronics & Drives*. IEEE, 2011, pp. 456–461.

[17] J. Petryna, A. Duda, and M. Sułowicz, "Eccentricity in induction machines—a useful tool for assessing its level," *Energies*, vol. 14, no. 7, p. 1976, 2021.

[18] G. E. Karniadakis, I. G. Kevrekidis, L. Lu, P. Perdikaris, S. Wang, and L. Yang, "Physics-informed machine learning," *Nature Reviews Physics*, vol. 3, no. 6, pp. 422–440, 2021.

[19] X. Zheng, B. Wang, D. Kalathil, and L. Xie, "Generative adversarial networks-based synthetic pmu data creation for improved event classification," *IEEE Open Access Journal of Power and Energy*, vol. 8, pp. 68–76, 2021.

[20] S. L. Brunton, J. L. Proctor, and J. N. Kutz, "Discovering governing equations from data by sparse identification of nonlinear dynamical systems," *Proceedings of the national academy of sciences*, vol. 113, no. 15, pp. 3932–3937, 2016.

[21] N. M. Mangan, S. L. Brunton, J. L. Proctor, and J. N. Kutz, "Inferring biological networks by sparse identification of nonlinear dynamics," *IEEE Transactions on Molecular, Biological and Multi-Scale Communications*, vol. 2, no. 1, pp. 52–63, 2016.

[22] D. L. Donoho, "For most large underdetermined systems of linear equations the minimal l1-norm solution is also the sparsest solution," *Communications on Pure and Applied Mathematics: A Journal Issued by the Courant Institute of Mathematical Sciences*, vol. 59, no. 6, pp. 797–829, 2006.

[23] S. Boyd, N. Parikh, and E. Chu, *Distributed optimization and statistical learning via the alternating direction method of multipliers*. Now Publishers Inc, 2011.

[24] R. G. D. Steel, J. H. Torrie *et al.*, "Principles and procedures of statistics." *Principles and procedures of statistics.*, 1960.